

ARCHIVES
of
FOUNDRY ENGINEERING



DOI: 10.2478/afe-2013-0069

ISSN (2299-2944)

Volume 13

Issue 3/2013

Published quarterly as the organ of the Foundry Commission of the Polish Academy of Sciences

101 – 106

Directional Solidification of Ledeburite

M. Trepczyńska-Lent

Faculty of Mechanical Engineering, University of Technology and Life Sciences
Kaliskiego 7, 85-796 Bydgoszcz, Poland

Corresponding author. E-mail address: malgorzata.trepczynska-lent@utp.edu.pl

Received 14.05.2013; accepted in revised form 27.05.2013

Abstract

Directional solidification of ledeburite was realised out using a Bridgman's device. The growth rate for movement sample $v=83.3 \mu\text{m/s}$ was used. In one sample the solidification front was freezing. The value of temperature gradient in liquid at the solidification front was determined. Interfacial distance λ on the samples was measured with NIS-Elements application for image analysis.

Keywords: Solidification process, Ledeburite, Directional solidification, Structure, Interfacial distance

1. Introduction

Eutectic solidification is frequently observed in metallic alloys, and has been intensively studied.

In the last years, the utilization of the directional solidification of eutectic alloys has been employed in a considerable number of experimental and theoretical investigation. The eutectic directional solidification provides us microstructures with the simultaneous formation of two solid phases from one determined liquid, i.e. the phases of interest are obtained directly from the melt. Directional solidification techniques provide several advantages in studying solidification reactions. Particular advantages of interest here are the ability to control the solidification velocity and examine microstructures of solidified alloys vs velocity; and by use of quenching, evaluation of the morphology of the solid/liquid interface and microstructural changes which occur by solid state reactions during cooling is possible. The experimental studies of alloys around the eutectic compositions of binary systems showed that in alloys frozen quickly, metastable phases are observed and formed with an eutectic morphology, being easily identified through metallographic analysis [1-9].

Parameter, influencing the kind of eutectic received, is the fraction of the volume g_a occupied by one of eutectic phases. Quasi-regular eutectic solidification near the highest value of g_a , which is over 0.4. They are characterized by lamellar-fibrous

morphology. Typical examples of this kind of eutectic can be seen in the Fe-Fe₃C, Bi-Cd, Sb-Cu₂Sb and Bi-Au₂Bi alloys. The characteristic of this group is that although they are in the anomalous (f-nf) class almost regular microstructures can be observed in these eutectics [10-13].

2. Solidification of ledeburite

Ledeburite is defined as the eutectic structure formed between Fe/Fe₃C. The term is used for both of the observed eutectic morphologies, i.e., rod ledeburite and plate ledeburite.

Ledeburite structures generally form in a two stage process. The first stage in the white iron formation was the growth of Fe₃C plate dendrites, just as in hypereutectic alloys; only in the hypoeutectic alloys, the Fe₃C dendrites grow around the pre-existing austenite dendrites.

In the second stage for both hyper- and hypoeutectic alloys, a cooperative eutectic growth of austenite and Fe₃C occurs on the sides of the primary Fe₃C plates as the liquid between the plates solidifies. The cooperative eutectic growth occurs at right angles to the primary Fe₃C plates, with the morphology being the very well-defined rod eutectic microstructure which is a dominant characteristic of white cast iron structures. In their model of the growth process, the initial edgewise is a noncooperative growth of primary Fe₃C dendrites leading the growth front [14].

During the side eutectic growth (x direction) the area of undercooling concentration of the liquid solution comes into being that leads to the destabilization of the front, which changes from the planar into cellular one. The growth of the cells leads to carbon enrichment in the intercellular niches, in which cementite can crystallize. Adjacent lamellar cementite shallows join together, the austenite shallow becomes distributed, plate eutectic changes into fibrous eutectic. During the further side growth of eutectic grains only fibrous eutectic still crystallizes. According to the observations, cementite eutectic changes into either continuous carbides phase with austenite inclusions, interpolation of various degree of dispersal, or plate structure that consists of the austenite and cementite plates [15].

After undercooling of cast iron below the cementite eutectic equilibrium temperature T_c , in the liquid alloy, cementite nuclei are created that take the form of plates during growth. On this plate, the austenite nucleates and grows in a dendritic form to cover the cementite (Fig. 1a).

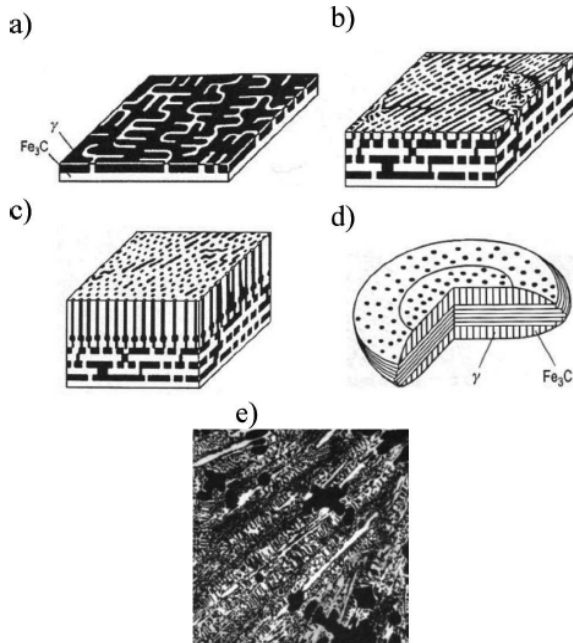


Fig. 1. Sequence of the development of cementite eutectic cell (a, b, c), a scheme of cell (d) and microstructure of a cross section of cementite eutectic cell (e) [10, 16]

A common solidification front of the eutectic structure is created. During its growth, plate-to-fibre transition of cementite takes place (Fig. 1 b, c) and a cell of cementite eutectic is formed (Fig. 1). In the central part of the cell, cementite takes the form of plates, while in the periphery, it assumes the form of fibres. Cross-section of eutectic cells in white cast iron (visible on metallographic specimens) is shown in Fig. 1e [16].

2.1. Interfacial distance in eutectic

Figure 2 is a schematic diagram of a regular lamellar eutectic structure which forms under steady-state directional solidification conditions for α , β phase [17, 18].

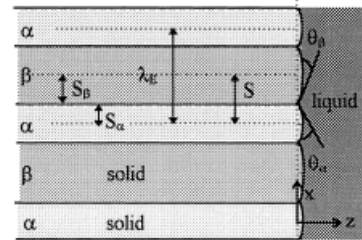


Fig. 2. A schematic diagram of a lamellar structure [4]

One of modelling of eutectic growth was given by Jackson and Hunt [18], why set up a mathematical model for stable growth of a regular eutectic with an isothermal growing interface, obtaining:

$$\lambda^2 v = \text{const} \quad (1)$$

where λ is the interfacial spacing, v is the growth rate.

For the irregular eutectics: extreme spacing - λ_e , minimum spacing - λ_m , maximum spacing - λ_M and average spacing - λ_a are described in Fig. 3.

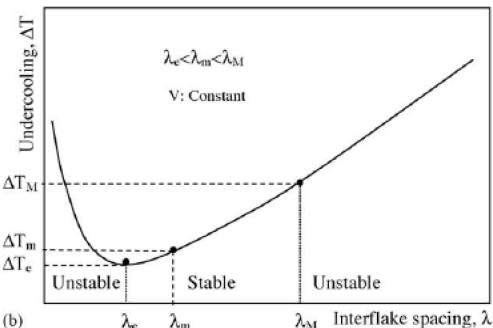


Fig. 3. The schematic plot of undercooling ΔT versus interflake spacing, λ for a given growth rate [7, 19]

The operating range can be described by the two dimensionless operating parameters, φ and η defined as:

$$\varphi = \frac{\lambda_a}{\lambda_e} = \frac{\lambda_m + \lambda_M}{2\lambda_e} \quad (2)$$

$$\eta = \frac{\lambda_M - \lambda_m}{\lambda_a} = \frac{2(\lambda_M - \lambda_m)}{\lambda_M + \lambda_m} \quad (3)$$

The φ value has been shown to be very well defined and independent of the growth rate. η is also independent of growth rate. The actual average spacing, λ_a , of irregular eutectic is larger than extremes spacing λ_e , so that the average eutectic spacing can

be characterized by Eq. (2) as, $\lambda_a = \varphi \lambda_e$, where φ is an operating parameter reflecting the spacing adjustment mechanism that is different from the minimum undercooling principles. φ value is much greater than unity whereas η is smaller than unity ($\eta < 1$) for irregular eutectics [7].

Most studies have shown that lamellar terminations are constantly created and move through the structure during eutectic growth. The presence and movement of faults and fault lines provide a means by which lamellar spacing changes can occur in response to growth rate fluctuations or a small growth rate change [19].

3. Experimental

Pre-study research was conducted to obtain an alloy of Fe-C with 4.3% contents of carbon. The obtained samples were a starting material to lead the research on directional solidification of ledeburite.

Armco iron and graphite electrodes with spectral purity were prepared as burden materials to the research.

Initial melting was done in Balzers - type vacuum heater, in the conditions of backing vacuum. The smelt was subsequently degassed under argon. The alloy was poured into four bar-shaped chills with a diameter $\varnothing 12$ mm. From prepared bars the samples of $\varnothing 5 \times 100$ mm were cut and then grinded.

The directional solidification of the alloy can be realized by many sorts of equipment. In the conducted tests Bridgman's method with vertical temperature gradient was applied. It means that the whole metal is melted and then the form is continuously pulled out of the heater straight to the cooling centre. Figure 4 shows the heater to directional solidification of alloys.

The machine consists of three main assemblies: a) resistor heating furnace, b) cooler, c) drive mechanism and additional supportive elements like power supply set, microprocessor supervising high temperature stabilization with an accuracy of $\pm 2^\circ\text{C}$ and required scope of crucible movements rates.

3.1. Measurement of temperature gradients

Kanthal Super resistance wire winding is a heating element (5) which ensures high temperature inside the furnace. A cooler (9) is built of two copper coats that takes care of continuous flow of water led to the thermostat. The space between internal coat and stall bar was fulfilled with low-melting alloy Ga-In-Sn with boiling high temperature. This alloy was used to eliminate gas gap between the crucible and a cooler and, as a result, to increase the temperature gradient in liquid metal at the front of solidification. In the upper part of alumina tube in upper head (1) the double pipe of Al_2O_3 with thermal element Pt40Rh-Pt20Rh (8) was installed.

It allows to record the temperature of liquid metal alongside its moving route, namely $T(x)$ where x is the distance from the cooler, as shown in Figure 5. On the basis of these data the curve

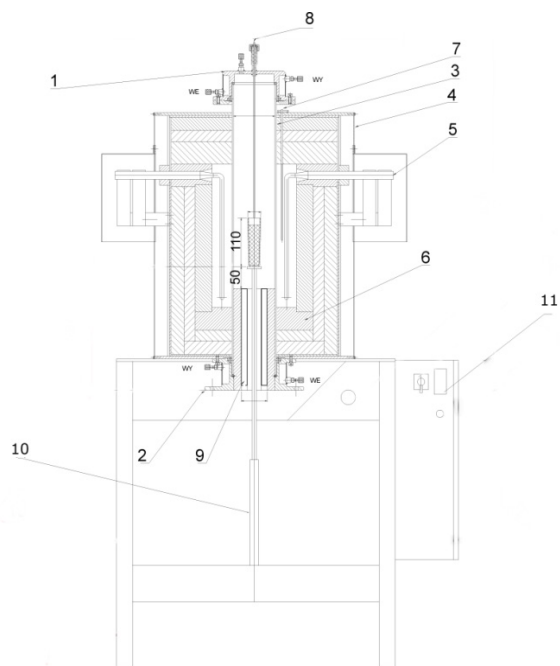


Fig. 4. Heater PPR-100/1650 to directional solidification with pointed elements and general dimensions. Marks: 1 – upper head; 2 – lower head; 3 – ceramic reactor; 4 – radiator case; 5 – heating element; 6 – high temperature fibrous isolation; 7 – regulatory thermal element; 8 – measurement thermal element; 9 – cooler, 10 – embarkation system; 11 – temperature regulator

of temperature uniformity was obtained and next, after numerical differentiation, the curve dT/dx (the uniformity of temperature gradient in the alloy) was determined. By using isotherm dividing liquid phase from solid one, the value of temperature gradient in the liquid at the front of solidification from the curve dT/dx , which is $G=33.5 \text{ K/mm}$ ($G=335 \text{ K/cm}$) (blue line).

Directional solidification was conducted in the following way. The samples of the initial alloy were placed inside alumina shields with a trade name Trialit-Degussit from Friatec Company with an internal diameter $\phi_w = 6 \text{ mm}$ and external diameter $\phi_z = 10 \text{ mm}$ and with a length 100 mm. These samples were stuck to the furnace drawbar by the high-temperature Morgan glue. The bottom end of the alumina shield and drawbar was submerged into liquid alloy fulfilling the cooler. After furnace sealing and delivering purified argon to the chamber the power was switched on. After the temperature stabilized to the level of 1450°C , the drive mechanism was launched. Drawbar with the samples on it was moving with a constant rate in regard to the cooler. On the determined temperature gradient at the front of solidification which is $G=33.5 \text{ K/mm}$ the sample movement rate of $v=83.3 \text{ }\mu\text{m/s}$ (300 mm/h). One of the samples after solidifying was immediately taken off the cooler (frozen). Fe-Fe₃C eutectic samples were unidirectionally solidified with a constant temperature gradient in order to study the dependence of average interfacial distance λ .

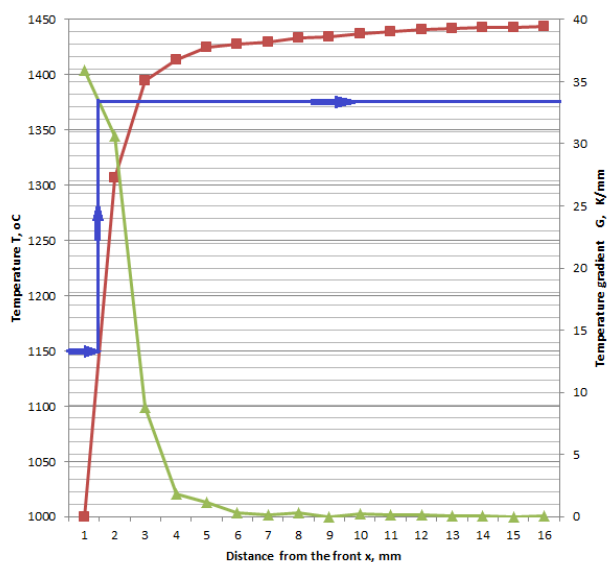


Fig. 5. Diagram of temperature gradient distribution in the examined alloy

3.2. Microstructure

After the process of directional solidification of eutectic alloy Fe-Fe₃C with sample movement rate of $v=83.3 \mu\text{m/s}$ the bars were obtained. On their longitudinal sections – in the different distance from the axis the metallographic specimens were made. The specimens were polished and etched with a reagent Nital. The Fig. 6. show the structure of ledeburite in the areas of obtained directional eutectic.

The structure of one sample which was frozen (immediately removed from the cooler) did not have the area of oriented ledeburite eutectic. Hypereutectic structure areas also appeared, namely ledeburite with numerous preliminary cementite separations, shown in Figure 7.

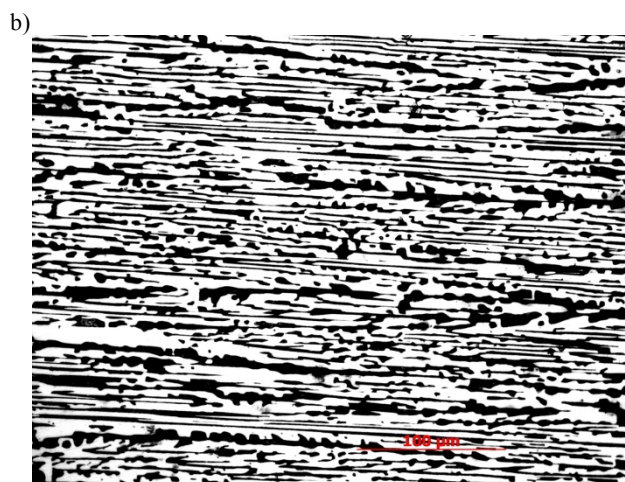
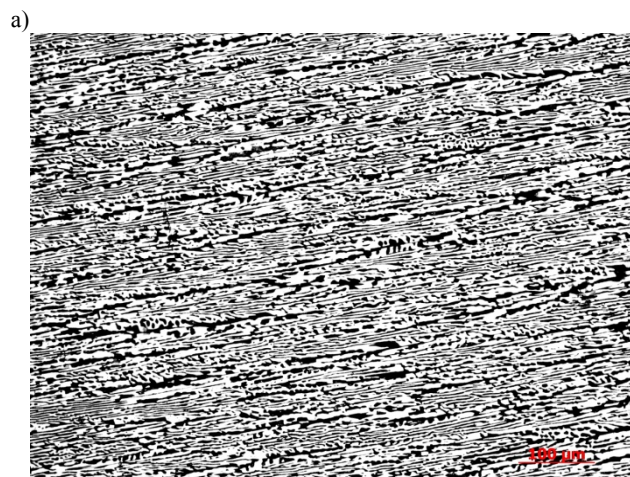


Fig. 6. Microstructure of directionally solidified ledeburite eutectic alloy on the longitudinal section of each samples, $G= 33.5 \text{ K/mm}$, a,b) $v=83.3 \mu\text{m/s}$

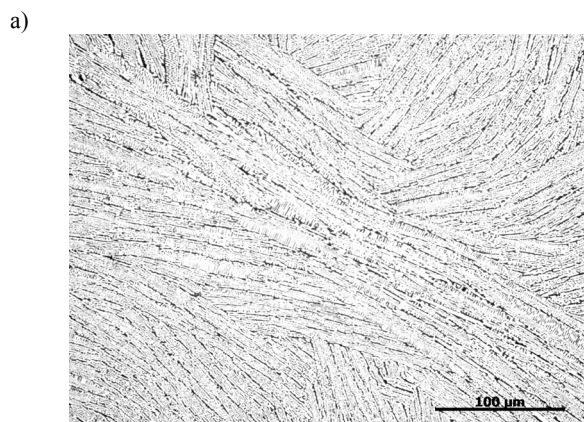


Fig. 7. Microstructure of a) eutectic, b) hypereutectic structure areas - samples after solidifying was frozen (immediately taken off the cooler), $v=83.3 \mu\text{m/s}$, $G= 33.5 \text{ K/mm}$

3.3. The measurement of interfacial distance

On the samples, where the eutectic was versed, the measurements of geometrical parameter λ were led.

In the literature concerning volume metallography [20, 21, 22] various methods of interfacial distance measurement in eutectic are suggested. In this case, the average interfacial distance in oriented cementite eutectic was determined as a quotient of measure lines $\sum L$ (perpendicular to the section) to the number of intersections f of these lines into cementite extraction:

$$\lambda = \frac{\sum L}{f} \quad (4)$$

Geometric parameter was measured also by using computer application to picture analysis NIS-Elements. On the straight, which was draw perpendicularly to the axis and the straight section, the distances between cementite separations were measured, as shown in the Figure 8.

Then, the calculations on the parameters were made with a use of Excel application. Approximately 240 lines, measured in at least 4 different distances from the face of the sample, in 5 successive longitudinal sections of each samples. The obtained values were verified statistically.

The measurements for average interfacial distance cementite eutectic was $8.25 \pm 0.52 \mu\text{m}$. Calculated value of $\lambda v^{1/2}$ was $75.3 \mu\text{m}^3 \text{s}^{-1/2}$.

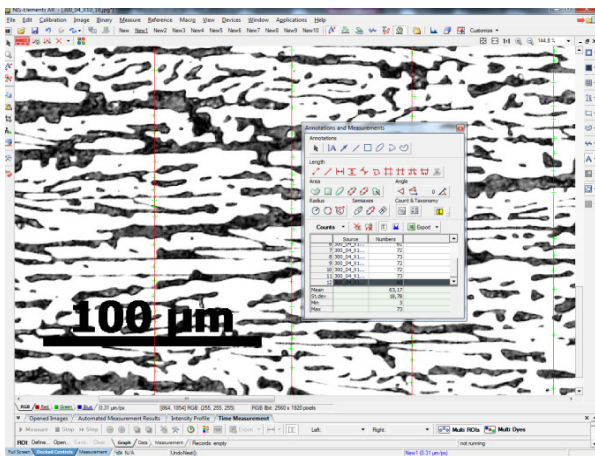


Fig. 8. Measurement method of the number of intersections f of these lines into cementite extraction

The dependence of average interfacial distance on distance from the face of the sample is shown in Fig. 9.

Figure 10 shows the topography directional ledeburite executed on the confocal microscope Lext OLS 4000.

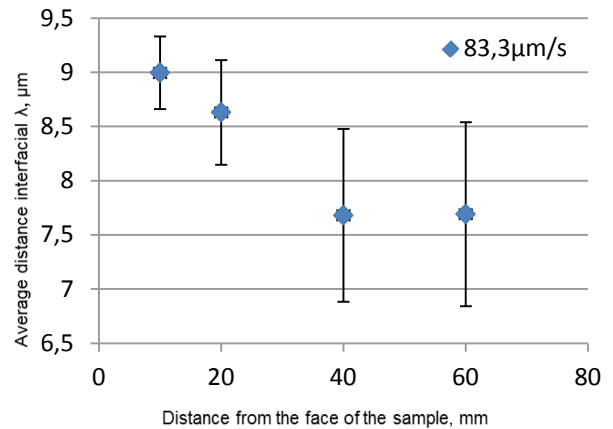


Fig. 9. The dependence of average interfacial distance λ on distance from the face of the sample, $G=33.5 \text{ K/mm}$

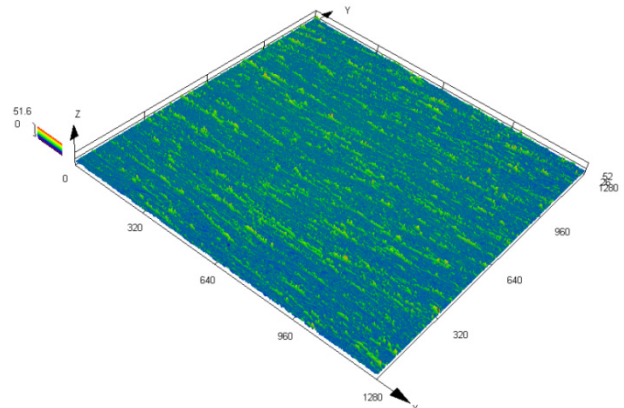


Fig. 10. Topography directional ledeburite ($v=83.3 \mu\text{m/s}$, $G=33.5 \text{ K/mm}$) executed on the confocal microscope Lext OLS 4000. Measuring the dimensions are given in μm

4. Conclusions

As a result of directional solidification of Fe-Fe₃C alloy with $v=83.3 \mu\text{m/s}$ and $G=33.5 \text{ K/mm}$, oriented ledeburite structure was obtained in some areas of the sample.

Interfacial distance were measured from longitudinal section of the directionally solidified eutectic samples. The average interfacial distance cementite eutectic was $8.25 \pm 0.52 \mu\text{m}$.

The structure of one sample which was frozen, did not have oriented ledeburite eutectic.

Acknowledgments

The directional solidification was realised in the Department of Casting at the AGH University of Science and Technology in Cracow. The author wishes to express his gratitude to Prof. E. Guzik, Ph.D. E. Olejnik and Ph.D. A. Janas from Faculty of Alloy Engineering and Casting Composition.

References

- [1] Aguiar, M.R. & Caram, R. (1996). Directional solidification of a Sn-Se eutectic alloy using the Bridgman-Stockbarger method. *Journal of Crystal Growth*. 166(1-4), 398-401. DOI: 10.1016/0022-0248(95)00524-2.
- [2] Magnin, P. & Trivedi, R. (1991). Eutectic growth: a modification of the Jackson and Hunt theory. *Acta Metall. Mater.* 39, 453-467. DOI: 10.1016/0956-7151(91)90114-G.
- [3] Kaya, H., Gündüz, M., Çadirli, E., Uzun, O. (2004). Effect of growth rate and lamellar spacing on microhardness in the directionally solidified Pb-Cd, Sn-Zn and Bi-Cd eutectic alloys. *Journal of Materials Science*. 1101. 39(21), 6571-6576. DOI: 10.1023/B:JMSC.0000044897.98694.be.
- [4] Cadirli, E. & Gündüz, M. (2000). The dependence of lamellar spacing on growth rate and temperature gradient in the lead-tin eutectic alloy. *Journal of Materials Processing Technology*. 97, 74-81. DOI: 10.1016/S0924-0136(99)00344-1.
- [5] Santos, I.A., Coelho, A.A., Araújo, R.C., Ribeiro, C.A., Gama, S. (2001). Directional solidification and characterization of binary Fe-Pr and Fe-Nd eutectic alloys. *Journal of Alloys and Compounds*. 325, 194-200. DOI: 10.1016/S0925-8388(01)01394-9.
- [6] Jones, H. & Kurz, W. (1981). Relation of interphase spacing and growth velocity in Fe-C and Fe-Fe₃C eutectic alloys. *Z. Metallkunde*. 72, 792-797.
- [7] Gündüz, M., Kay, H., Cadirli, E., Ozme, A. (2004). Interflake spacings and undercoolings in Al-Si irregular eutectic alloy. *Material Science and Engineering A*(3690), 215-229. DOI: 10.1016/j.msea.2003.11.020.
- [8] Guzik, E. (1994). *A model of irregular eutectic growth taking as an example the graphite eutectic in Fe-C alloys*. Dissertations Monographies 15, Cracow: AGH Publ.
- [9] Guzik, E. & Kopyciński, D. (2006). Modelling structure parameters of irregular eutectic growth: Modification of Magnin-Kurz theory. *Metallurgical and Materials Transactions A*. 37(A), 3057-3067. DOI: 10.1007/s11661-006-0187-7.
- [10] Fraś, E. (2003). *Crystallization of metals*. Warsaw: WNT.
- [11] Savas, M.A. & Smith, R.W. (1985). Quasi-regular growth: a study of the solidification of some high volume-fraction faceted phase anomalous eutectics. *Journal of Crystal Growth*. 71, 66-74. DOI: 10.1016/0022-0248(85)90044-2.
- [12] Trepczyńska-Lent, M. (2007). Solidification of quasi-regular eutectic. *Archives of Foundry Engineering*. 7(3), 171-178.
- [13] Trepczyńska-Lent, M. (2012). Solidification of ledeburite eutectic. *Archives of Foundry Engineering*. 12(spec. 2), 71-74.
- [14] Park, J.S. & Verhoeven, J.D. (1996). Directional solidification of white cast iron. *Metallurgical and Materials Transactions A*. 27(A), 2328-2337. DOI: 10.1007/BF02651887.
- [15] Podrzućki, Cz. (1991). *Cast iron. Structure, properties, application*. Cracow: ZG STOP.
- [16] Fraś, E. & Górny, M. (2012). An inoculation phenomenon in cast iron. *Archives of Metallurgy and Materials*. 57(3), 767-777. DOI: 10.2478/v10172-012-0084-6.
- [17] Ludwig, A. & Leibbrandt, S. (2004). Generalized Jackson-Hunt model for eutectic solidification at low and large Peclet numbers and any binary eutectic phase diagram. *Material Science and Engineering A*, 540-546. DOI: 10.1016/j.msea.2003.10.108.
- [18] Jackson, K.A. & Hunt, J.D. (1966). Lamellar and rod eutectic growth. *Trans. Metall. Soc. AIME*. 236, 1129-1142.
- [19] Cadirli, E., Kaya, H., Gündüz, M. (2003). Effect of growth rates and temperature gradients on the lamellar spacing and the undercooling in the directionally solidified Pb-Cd eutectic alloy. *Materials Research Bulletin*. 38, 1457-1476. DOI: 10.1016/S0025-5408(03)00169-7.
- [20] Ryś, J. (1983). *Quantitative metallography*. Cracow: AGH Publ.
- [21] Sołtykow, S.A. (1976). *Stereometričeskaja mietallografija*. Moscow: Miedalurgija Publ.
- [22] Fraś, E. (1981). *Solidification of cast iron*. Script AGH. Cracow. 811.